

GLOBAL STRINGS IN EXTRA DIMENSIONS: A FULL MAP OF SOLUTIONS, MATTER TRAPPING, AND THE HIERARCHY PROBLEM

K.A. Bronnikov^{1†} and B.E. Meierovich^{2‡}

[†] *Center for Gravitation and Fundamental Metrology, VNIIMS,*

46 Ozyornaya St., Moscow 119361, Russia;

Institute of Gravitation and Cosmology, PFUR, 6 Miklukho-Maklaya St., Moscow 117198, Russia

[‡] *Kapitza Institute for Physical Problems, 2 Kosygina St., Moscow 117334, Russia*

We consider $(d_0 + 2)$ -dimensional configurations with global strings in the two extra dimensions and a flat metric in d_0 dimensions, endowed with a warp factor $e^{2\gamma}$ depending on the distance l from the string center. All possible regular solutions to the field equations are classified by the behavior of the warp factor and the extra-dimensional circular radius $r(l)$. Solutions with $r \rightarrow \infty$ and $r \rightarrow \text{const} > 0$ as $l \rightarrow \infty$ are interpreted in terms of thick brane world models. Solutions with $r \rightarrow 0$ as $l \rightarrow l_c > 0$, i.e., those with a second center, are interpreted as either multi-brane systems (which is appropriate for large enough distances l_c between the centers) or as Kaluza-Klein type configurations with extra dimensions invisible due to their smallness. For the case of the Mexican-hat symmetry breaking potential, we build a full map of regular solutions on the (ε, Γ) parameter plane, where ε acts as an effective cosmological constant while Γ characterizes the gravitational field strength. The trapping properties of candidate brane worlds for test scalar fields are discussed. Good trapping properties for massive fields are found for models with growing warp factors. Kaluza-Klein type models are shown to possess nontrivial warp factor behaviors, leading to matter particle mass spectra which seem promising from the standpoint of hierarchy problems.

PACS: 04.50.+h, 11.27.+d

1. Introduction

The multidimensional gravity concept, tracing back to the pioneering papers by Kaluza and Klein [1], initially assumed that the extra dimensions remain unobservable due to their extreme smallness. Another class of multidimensional theories has been put forward in the 80s, on the basis of the idea that we live on a distinguished surface (brane) embedded in a higher-dimensional manifold, called the bulk [2]. This idea has recently become very popular in attempts to find an approach to a number of fundamental physical problems. The brane-world concept is broadly discussed in connection with the recent developments in supersymmetric string/M-theories [3]. The simple RS1 model [4] has continued numerous attempts [5] to find the origin of the enormous hierarchy of energy/mass scales observed in nature, which is a long-standing problem in particle physics. In astrophysics and cosmology, there are attempts to explain the dark matter and dark energy effects, to describe black holes and possible variation of fundamental constants, the CMB anisotropy etc.

A great variety of brane world models may be found in the literature: branes in 5 or more dimensions, single or multiple branes, flat or curved branes, flat or curved bulk, compact or non-compact bulk (i.e., large or infinite extra dimensions), thin or thick branes, various symmetries of both bulks and branes, different kinds of matter forming the brane etc.

In our view, the most natural physical idea leading to the emergence of distinguished surfaces in the space-time manifold is the idea of a phase transition with spontaneous symmetry breaking (SSB) which has already led to great success in many areas of physics and cosmology. In other words, it is reasonable to consider the brane world as a result of a phase transition at a very early stage of the Universe evolution. The existing macroscopic theory of phase transitions with SSB allows one to consider the brane world concept self-consistently and maximally escape the influence of model assumptions even without a detailed knowledge of the nature of physical vacuum. A necessary consequence of such phase transitions is the appearance of topological defects.

Let us recall that a decisive step toward cosmological applications of the SSB concept was made in 1972 by Kirzhnits [6]. He assumed that, as in the case of solid substances, a symmetry of a field system, existing at sufficiently high temperatures, could be spontaneously broken as the temperature falls down. The first quantitative analysis of the cosmological consequences of SSB was given by Zel'dovich, Kobzarev, and Okun' [7].

The properties of global topological defects are generally described with the aid of a multiplet of scalar fields playing the role of an order parameter. If a defect is to be interpreted as the origin of a brane world, its structure is determined by the self-gravity of a scalar field system and may be described by a set of Einstein and scalar equations.

This approach to the brane-world concept has been employed by many authors for construction of thick branes in five (see, e.g., [8–14]) and more (see, e.g., [15–18] and references therein) dimensions.

In our previous papers [13, 14, 17, 18], we have analyzed the gravitational properties of candidate (thick) brane worlds with the d_0 -dimensional Minkowski metric and global topological defects in $d_1 + 1$ extra dimensions. Our general formulation covered such particular cases as a brane (domain wall) in five-dimensional spacetime (one extra dimension), a global cosmic string with winding number $n = 1$ (two extra dimensions), and global monopoles (three or more extra dimensions). We restricted ourselves to Minkowski branes since most of the existing problems are clearly seen even in these comparatively simple systems; on the other hand, in the majority of physical situations, the intrinsic curvature of the brane itself is much smaller than the curvature related to brane formation, and therefore the main qualitative features of Minkowski branes should survive in realistic curved branes.

Our treatment differed from many others (e.g., [15, 16]) in that we have considered all kinds of regular solutions to the corresponding field equations, including those with growing warp factors, and have emphasized good trapping properties of the latter.

We have shown, in particular, that there are as many as seven classes of regular solutions of the field equations describing global strings and monopoles in extra dimensions; two of them exist for monopoles only while the other five are found for both strings and monopoles. Some of these configurations have exponentially growing warp factors ($e^{2\gamma}$ in the metric (1), see below) at large distances from the core. They are shown to trap linear test scalar fields of any mass and momentum. Others, ending with a flat metric, have a warp factor tending to a constant value, determined by the shape of the symmetry breaking potential. They are also shown to trap test scalar fields with masses bounded above by a value depending on the particular parameters of the topological defect.

Though the general classification of [17, 18] covers all possible regular configuration, the important question of location of different solutions in the space of physical parameters remained open. One of the goals of this paper is to answer this question for the particular case of a global string in

two extra dimensions and a Mexican-hat symmetry breaking potential. The problem then contains two essential physical parameters: ε , the dimensionless cosmological constant, and Γ , characterizing the gravitational field strength. The border lines in the (ε, Γ) plane, separating different classes of regular solutions (those extending to infinite circular radii r , those with a cylindrical geometry far from the center and those with two regular centers), are found numerically, and the asymptotic dependences $\varepsilon(\Gamma)$ as $\Gamma \rightarrow 0$ and $\Gamma \rightarrow \infty$ are derived analytically.

Another goal is to give a more complete description of the configurations of interest described by these solutions. Thus, we describe the trapping properties of different thick brane world models for classical particles, scalar fields and gravity. We also argue that one of the classes of regular configurations, those with two centers, can lead to promising models with nontrivial particle mass spectra. The point is that the warp factors of such configurations can have several minima at different levels, where test particles and fields may be gravitationally trapped with different energies. Though, in this case, one should abandon the brane world concept and admit that the extra dimensions are invisible due to their smallness, i.e., interpret the solutions in the spirit of Kaluza-Klein theories.

There is a growing number of publications devoted to brane worlds with two extra dimensions, see [19] and references therein. In many cases the results are obtained numerically using simplified models with specially chosen sets of parameters. In our macroscopic approach, based on the theory of phase transitions with SSB, we try to reduce the influence of model assumptions to a minimum and to cover the full range of opportunities. Our main result, the full map of regular solutions for a system with the Mexican-hat symmetry-breaking potential $V(\phi)$, should probably retain its basic qualitative features for other potentials with a similar disposition of extremum points.

The paper is organized as follows. Sec. 2 outlines the problem setting, including the geometry, field equations and boundary conditions providing space-time regularity. Sec. 3 describes the simplest solutions with a constant scalar field, needed for comparison in what follows. Sec. 4 is central in the paper: we give a general description and classification of possible regular solutions on the basis of our previous work [17, 18] and present a map showing the location of different solutions with the Mexican hat potential in the parameter space of the problem. In Sections 5 and 6 we describe some further details of the solutions and give an analytic derivation of the asymptotic behavior of the curves drawn in the map. Sec. 8 discusses the trapping properties of thick branes described by the above solutions. Sec. 9 outlines the properties of configurations with two centers, and Sec. 10 is a conclusion.

2. Problem setting

2.1. Geometry and regularity conditions

Our main interest here is 6D space-time with a cosmic string in the two extra dimensions. Let us, however, begin with a more general geometry: consider a $(D = d_0 + d_1 + 1)$ -dimensional space-time with the structure $\mathbb{M}^{d_0} \times \mathbb{R}_u \times \mathbb{S}^{d_1}$ and the metric

$$ds^2 = e^{2\gamma(u)} \eta_{\mu\nu} dx^\mu dx^\nu - (e^{2\alpha(u)} du^2 + e^{2\beta(u)} d\Omega^2). \quad (1)$$

where $\eta_{\mu\nu} = \text{diag}(1, -1, \dots, -1)$ is the d_0 -dimensional Minkowski metric ($d_0 > 1$), $d\Omega$ is a linear element on a d_1 -dimensional unit sphere \mathbb{S}^{d_1} , α , β and γ are functions of the radial coordinate u with the definition domain $\mathbb{R}_u \subseteq \mathbb{R}$ to be specified later. We will also use the notation $r \equiv e^\beta$ where r is the spherical (circular for $d_1 = 1$) radius.

The Riemann tensor $R^{AB}{}_{CD}$ is diagonal with respect to pairs of indices and has the nonzero components

$$R^{\mu\nu}{}_{\rho\sigma} = -e^{-2\alpha} \gamma'^2 \delta^{\mu\nu}{}_{\rho\sigma},$$

$$\begin{aligned}
R^{ab}_{cd} &= (e^{-2\beta} - e^{-2\alpha}\beta'^2)\delta^{ab}_{cd}, \\
R^{u\mu}_{uv} &= -\delta^\mu_\nu e^{-\gamma-\alpha}(e^{\gamma-\alpha}\gamma')', \\
R^{ua}_{ub} &= -\delta^a_b e^{-\beta-\alpha}(e^{\beta-\alpha}\beta')', \\
R^{a\mu}_{b\nu} &= -\delta^\mu_\nu \delta^a_b e^{-2\alpha}\gamma'\beta'.
\end{aligned} \tag{2}$$

where $\delta^{\mu\nu}_{\rho\sigma} = \delta^\mu_\rho \delta^\nu_\sigma - \delta^\mu_\sigma \delta^\nu_\rho$ and similarly for other indices. The indices μ, ν, \dots correspond to d_0 -dimensional (physical) space-time, a, b, \dots to d_1 angular coordinates on \mathbb{S}^{d_1} , and A, B, \dots to all D coordinates.

A necessary condition of regularity is finiteness of all algebraic invariants of the Riemann tensor. In our case it is sufficient to deal with the Kretschmann scalar $K = R^{AB}_{CD}R^{CD}_{AB}$ since it is a sum of squares of all nonzero R^{AB}_{CD} . Hence, in regular configurations all components of the Riemann tensor (2) are finite.

In the Gaussian gauge $\alpha = 0$, $u = l$ being the proper distance along the radial direction, the regularity conditions at $r > 0$ look very simple:

$$\beta', \quad \beta'', \quad \gamma', \quad \gamma'' \quad \text{should be finite.} \tag{3}$$

The regularity conditions at the center $r = 0$ follow from finiteness of the Riemann tensor components R^{ab}_{cd} and coincide with the regular center conditions in usual static, spherically symmetric metrics. In terms of an arbitrary u coordinate, the regular center conditions are

$$\gamma = \gamma_c + O(r^2) \quad e^{\beta-\alpha}|\beta'| = 1 + O(r^2) \quad \text{as } r \rightarrow 0. \tag{4}$$

The latter condition means a correct ($= 2\pi$) circumference to radius ratio, or, equivalently, $dr^2 = dl^2$; γ_c is a constant which can be set to zero by rescaling the coordinates x^μ .

The string case $d_1 = 1$ has a specific feature: there is only one angular coordinate, therefore $\delta^{ab}_{cd} \equiv 0$, hence $R^{ab}_{cd} \equiv 0$. However, a conical singularity is possible (i.e., an angular deficit, $dr^2 < dl^2$, or excess, $dr^2 > dl^2$), which is a pointwise, delta-like curvature peak over this zero level, as in the case of an ordinary cone top. Its existence actually means that there is some pointlike object with respect to the two extra dimensions, or a thin brane in the space-time as a whole.

Below we will consider entirely regular configurations, excluding, among others, conical singularities.

2.2. Topological defects. Field equations

A global defect with a nonzero topological charge can be constructed with a multiplet of $d_1 + 1$ real scalar fields ϕ^k , in the same way as, e.g., in [17]. It comprises a ‘‘hedgehog’’ configuration in $\mathbb{R}_u \times \mathbb{S}^{d_1}$:

$$\phi^k = \phi(u)n^k(x^a),$$

n^k is a unit vector in the $d_1 + 1$ -dimensional Euclidean target space of the scalar fields: $n^k n^k = 1$.

The total Lagrangian of the system is taken in the form

$$L = \frac{R}{2\kappa^2} + \frac{1}{2}g^{AB}\partial_A\phi^k\partial_B\phi^k - V(\phi), \tag{5}$$

where R is the D -dimensional scalar curvature, κ^2 is the D -dimensional gravitational constant, and V is a symmetry-breaking potential depending on $\phi^2(u) = \phi^a\phi^a$.

The case $d_1 = 0$, with only one extra dimension, is a flat domain wall. Regular thick Minkowski branes supported by scalar fields with arbitrary potentials were analyzed in [13, 14].

The case $d_1 = 1$ is a global cosmic string with the winding number $n = 1$, to be discussed here in detail. In case $d_1 > 2$ we have a global monopole in the extra space-like dimensions, see, e.g., [15–18, 20, 21].

Let us write down the scalar field equation and three components of the Einstein equations for such systems in the Gaussian gauge $\alpha = 0$, $u = l$ (the prime denotes d/dl):

$$\phi'' + (d_0\gamma' + d_1\beta'^2)\phi' - d_1 e^{-2\beta}\phi = \frac{\partial V}{\partial\phi}, \quad (6)$$

$$\gamma'' + d_0\gamma'^2 + d_1\beta'\gamma' = -\frac{2\kappa^2}{D-2}V, \quad (7)$$

$$\beta'' + d_0\beta'\gamma' + d_1\beta'^2 = (d_1 - 1 - k^2\phi^2)e^{-2\beta} - \frac{2\kappa^2}{D-2}V, \quad (8)$$

$$(d_1\beta' + d_0\gamma')^2 - d_0\gamma'^2 - d_1\beta'^2 = \kappa^2(\phi'^2 - 2V) + d_1 e^{-2\beta}(d_1 - 1 - \kappa^2\phi^2). \quad (9)$$

Any three of the above four equations are independent, and the fourth one is their consequence.

2.3. Boundary conditions and fine-tuning relations

The metric can be rewritten in the form

$$ds^2 = e^{2\gamma(l)}\eta_{\mu\nu}dx^\mu dx^\nu - dl^2 - r^2(l)d\Omega^2, \quad (10)$$

where $r = e^\beta$ is the spherical radius. Assuming that there is a regular center ($r = 0$), we put there $l = 0$ without loss of generality, and we will classify the configurations under study by the limiting value of $r(l)$ (infinite, finite, or zero) at the largest or infinite values of l .

In the general monopole case, the regular center requirement leads to the following boundary conditions for Eqs. (6)–(9) at $l = 0$:

$$\phi(0) = \gamma'(0) = r(0) = 0, \quad r'(0) = 1. \quad (11)$$

The system (6)–(9) does not contain γ but only its derivatives. It is convenient for numerical integration to work with Eqs. (6)–(8) solved with respect to the second-order derivatives and consider (9) as their first integral.

We thus have four boundary conditions (11) for the (effectively) fourth-order set of equations. It might seem that we must obtain a unique solution. However, this is not the case since $l = 0$, being a singular point of the spherical coordinate system (not to be confused with a space-time curvature singularity), is also a singular point of our set of equations. As a result, our set of equations admits an additional freedom of choosing $\phi'(0)$; or, instead, we may use the requirement of global regularity to obtain a unique solution.

Infinite extra dimensions

If the solution is defined in the interval $0 \leq l < \infty$, then the lacking boundary condition can be taken as $\phi \rightarrow \text{const}$ as $l \rightarrow \infty$, or

$$\phi'(\infty) = 0. \quad (12)$$

In general, when the scalar field starts from a maximum of the potential and ends at a finite value of ϕ , the five boundary conditions (11) and (12) uniquely determine a nontrivial solution to our field equations. Its existence determines a certain area in the space of parameters of the problem

without *a priori* fine tuning. An asymptotic analysis at $l \rightarrow \infty$ shows that in this general case $\beta(l)$ is a linearly growing function as $l \rightarrow \infty$, and $r'(\infty) \geq 0$.

$r'(\infty) = 0$ is the special case when r tends to a finite constant at $l \rightarrow \infty$. The solution then terminates at a slope of the potential rather than its minimum. The supplementary condition $r'(\infty) = 0$ seems to require a fine tuning relation between the free parameters of the problem. But we shall see that it is not quite so. An analysis of solutions with $\phi = \phi_0 = \text{const}$ shows that there is also an area in the parameter space where the condition (12) is fulfilled automatically, and solutions with $r'(l) \rightarrow 0$ as $l \rightarrow \infty$ exist without any fine tuning.

Two centers

It can happen that the integral curves of a solution terminate at some finite value l_c with $r(l_c) = 0$ and $\phi(l_c) = 0$, which is one more center. Of interest for us are configurations in which this second center $l = l_c$ is also regular. Then the same four conditions (11) should hold at $l = l_c$ too. Two of them can be fulfilled by choosing the values of $\phi'(0)$ and l_c . Two others can only be fulfilled by a proper choice of free (input) parameters of the problem, e.g., those of the potential (if any) and the cosmological constant.

In the special case of symmetry between the centers¹, the input parameters are connected by only one fine-tuning relation. In this case, the boundary conditions at the second center are satisfied automatically, and the existence of a regular solution is provided by three conditions of smoothness at the middle (equator) point $l_{\text{eq}} = l_c/2$:

$$\phi'(l_{\text{eq}}) = \gamma'(l_{\text{eq}}) = r'(l_{\text{eq}}) = 0.$$

Two of these three conditions determine the values of l_c and $\phi'(0)$, and the remaining one requires fine tuning of the input parameters of the problem.

The fine tuning could be avoided at the expense of admitting conical singularities (in the string case) at the two centers. For symmetric solutions the three smoothness conditions at the equator could be satisfied by choosing $\phi'(0)$, $r'(0)$ and l_c . In the general case of nonsymmetric centers, the four conditions of the second center could be satisfied by appropriately choosing $\phi'(0)$, $r'(0)$, $r'(l_c)$ and l_c .

¹Eqs. (6)–(9) are invariant under translations $l \rightarrow l + l_0$ and under reflections $l_0 + l \rightarrow l_0 - l, \phi \rightarrow -\phi$. This invariance gives rise to existence of regular solutions with two centers, which are symmetric against the middle point [17].

Furthermore, a solution with two regular centers defined in the interval $(0, l_c)$ can be symmetrically extended to the next interval $(l_c, 2l_c)$ and further on, thus leading to a periodic solution for $l \in \mathbb{R}$ [22]. The metric remains regular everywhere; however, the points of contacts $(0, \pm l_c, \pm 2l_c, \dots)$ are geometrically ambiguous: each of them belongs to two adjacent manifolds simultaneously.

If one still believes in the reality of such systems, one can note that the spectrum of a low-energy particle in a perfectly periodic potential has a conductivity zone, allowing free propagation and thus making the extra dimension observable in principle. However, if the conductivity zone is very narrow, then even small perturbations should lead to localization of a particle. This interesting new possibility is worth a special consideration.

2.4. String equations

In the string case $d_1 = 1$ to be considered here in detail, the field equations take the form

$$\phi'' + (d_0\gamma' + \beta'^2)\phi' - e^{-2\beta}\phi = \frac{\partial V}{\partial\phi}, \quad (13)$$

$$\gamma'' + d_0\gamma'^2 + \beta'\gamma' = -\frac{2\chi^2}{d_0}V, \quad (14)$$

$$\beta'' + d_0\beta'\gamma' + \beta'^2 = -(\chi^2\phi^2)e^{-2\beta} - \frac{2\chi^2}{d_0}V, \quad (15)$$

$$2d_0\gamma'\beta' + d_0(d_0 - 1)\gamma'^2 = \chi^2(\phi'^2 - 2V) - \chi^2\phi^2e^{-2\beta}. \quad (16)$$

For numerical examples, we will use the so-called Mexican hat potential

$$V = \frac{1}{4}\lambda_0\eta^4\left[\varepsilon + \left(1 - \frac{\phi^2}{\eta^2}\right)^2\right]. \quad (17)$$

The parameter ε plays the role of a cosmological constant added to the conventional Mexican hat potential (the ‘‘hat’’ is thus moved up or down). To pass to dimensionless quantities, we put $\lambda_0\eta^2 = 1$, so that lengths will be measured in units of $1/(\sqrt{\lambda_0}\eta)$ which in many cases has the meaning of the string core radius².

The potential then takes the form

$$V = \frac{1}{4}\eta^2[\varepsilon + (1 - f^2)^2], \quad f := \frac{\phi}{\eta}. \quad (18)$$

The remaining free parameters that control the system behavior are

$$d_0, \quad \varepsilon, \quad \text{and} \quad \Gamma := \chi^2\eta^2. \quad (19)$$

We will use $d_0 = 4$ in computations. The parameter Γ characterizes the gravitational field strength.

In the further description of different regular solutions to our field equations, we begin with the simplest solutions in which $\phi = \phi_* = \text{const}$. They are not string solutions but are helpful for comparison.

3. Solutions with $\phi = \text{const}$

If $\phi = \phi_* = \text{const}$, we are actually dealing with vacuum field equations for the metric (10) with the cosmological constant $\Lambda = \chi^2V(\phi_*)$.

The scalar field equation (13) reduces to

$$\phi_*/r^2 = -V_\phi(\phi_*), \quad V_\phi := dV/d\phi. \quad (20)$$

This leads to two kinds of solutions: one exists in the case $V_\phi(\phi_*) = 0$, $\phi_* = 0$, the other corresponds to $V_\phi(\phi_*) \neq 0$ (i.e., ϕ is ‘‘frozen’’ on a slope of the potential), and in this case we should put $r = \text{const}$.

For the potential (17), Eq. (20) gives

$$f_*(r^{-2} - 1 + f_*^2) = 0, \quad (21)$$

so that either $f_* = \phi_*/\eta = 0$ or $f_*^2 = 1 - 1/r^2$.

²From the very beginning, we put $c = \hbar = 1$, so that all quantities are measured in appropriate powers of length $[\ell]$. Then some relevant dimensionalities are $[V] = [\ell^{-D}]$, $[\phi^2] = [\eta^2] = [\chi^{-2}] = [\ell^{2-D}]$.

3.1. Solutions with $\phi \equiv 0$

The trivial regular solutions with the order parameter $\phi \equiv 0$ describe configurations with a higher symmetry, which can become spontaneously broken into a structure with a topological defect.

In this case the metric obeys the equations

$$\begin{aligned}\gamma'' + \gamma'(d_0\gamma' + \beta') &= -8\Lambda/d_0, \\ \beta'' + \beta'(d_0\gamma' + \beta') &= -8\Lambda/d_0, \\ (d_0 - 1)\gamma'^2 + 2\gamma'\beta' &= -8\Lambda/d_0.\end{aligned}\tag{22}$$

Excluding β' , we get the equation for γ

$$\gamma'' + \frac{1}{2}(d_0 + 1)\gamma'^2 + \frac{4\Lambda}{d_0} = 0\tag{23}$$

Its solutions are different for positive and negative Λ . For $\Lambda > 0$ we get (requiring $\gamma(0) = \gamma'(0) = 0$ — a regular center at $l = 0$)

$$e^{(d_0+1)\gamma} = \cos^2(\lambda_1 l), \quad \lambda_1 = \sqrt{2\Lambda \frac{d_0 + 1}{d_0}}.\tag{24}$$

The last equation (22) then gives for $r = e^\beta$:

$$r^2 = r_0^2 e^{-(d_0-1)\gamma} \sin^2(\lambda_1 l), \quad r_0 = \text{const},\tag{25}$$

where, choosing $r_0 = 1/\lambda_1$, we can satisfy the regularity condition $r'(0) = 1$. We thus have a configuration with a regular center but with a singularity $e^\gamma \rightarrow 0$ and $r \rightarrow \infty$ as $l \rightarrow \pi/(2\lambda_1)$.

For the potential (17), this case corresponds to $\varepsilon > -1$.

For $\Lambda < 0$, corresponding to $\varepsilon < -1$, we have, instead of (24) and (25)³,

$$e^\gamma = \cosh^{2/(d_0+1)}(\lambda_2 l), \quad \lambda_2 = \sqrt{-2\Lambda \frac{d_0 + 1}{d_0}}.\tag{26}$$

$$r = r_0 \frac{\sinh(\lambda_2 l)}{[\cosh(\lambda_2 l)]^{(d_0-1)/(d_0+1)}},\tag{27}$$

and again, choosing $r_0 = 1/\lambda_2$, we can satisfy the regularity condition $r'(0) = 1$.

So the configuration with unbroken symmetry is completely regular and extends from the regular center $l = 0$ to $l = \infty$ where the warp factor $e^{2\gamma}$ and the radius r are infinitely growing functions.

3.2. Solution with $\phi = \phi_* = \text{const} \neq 0$

In this case, Eq. (20) leads to a constant radius $r = r_*$, and Eq. (15) gives the relation

$$\phi_*^2/r_*^2 = -V(\phi_*)/d_0,\tag{28}$$

whence it follows $V(\phi_*) = \Lambda/\varkappa^2 < 0$.

For γ we get from (16)

$$d_0^2 \gamma'^2 = -2\Lambda, \quad e^{d_0 \gamma} = e^{\pm\sqrt{-2\Lambda}l},\tag{29}$$

³For $d_0 = 4$ these formulae reduce to those found earlier in [23].

Table 1: Classification of regular $(d_0 + 2)$ -dimensional solutions for arbitrary $V(\phi)$ by the types of asymptotic behavior at the largest or infinite l . The columns denoted r , ϕ , and γ show their final values. Attraction or repulsion is meant with respect to the center. The symbol η means a minimum of $V(\phi)$.

Notation	l range	r	ϕ	$V(\phi)$	γ	Asymptotic type
A0	\mathbb{R}_+	∞	$\equiv 0$	$V(0) < 0$	∞	AdS, attraction
A1	\mathbb{R}_+	∞	η	$V(\eta) < 0$	∞	AdS, attraction
A2	\mathbb{R}_+	∞	0	0	∞	power-law, attraction
B0	\mathbb{R}	$\equiv r_*$	$\equiv \phi_* \neq 0$	$V_* < 0$	$\pm\infty$	horizon at one end
B1	\mathbb{R}_+	r_*	$\phi_* \neq 0$	$V_* < 0$	$-\infty$	horizon, repulsion
B2	\mathbb{R}_+	r_*	$\phi_* \neq 0$	$V_* < 0$	∞	attracting tube
C	$(0, l_c)$	0	0	$V(0) > 0$	const	second center

and the coordinate range is $l \in \mathbb{R}$. In particular, for the potential (17) we have from (21) and (15)

$$r = 1/\sqrt{1 - f_*^2} = \text{const}, \quad (30)$$

$$\varepsilon = -2d_0(1 - f_*^2)f_*^2 - (1 - f_*^2)^2 < 0, \quad (31)$$

$$\Lambda = \varkappa^2 V(\phi_*) = -\frac{1}{2}\varkappa^2 \eta^2 d_0 f_*^2 (1 - f_*^2). \quad (32)$$

The configurations with $\phi = \text{const} \neq 0$ and $r = \text{const}$ are regular but evidently cannot be interpreted in terms of a brane world. They only provide the asymptotic behavior of the “tube” solutions presented below.

4. Regular string solutions. Classification and map in the (Γ, ε) plane

The possible types of regular solutions to our field equations have been classified in Refs. [17, 18]. Table 1 represents this classification for the string case $d_1 = 1$. Compared to [17], this table omits the solutions existing only for $d_1 > 1$, but additionally includes the solutions (labelled A0 and B0) from Sec. 3.

In what follows, we will deal with the potential (18). For this potential, Fig. 1 presents the location of different regular string solutions in the plane of parameters (Γ, ε) . The map shows solutions with the ϕ field having a constant sign. Those with alternate signs of ϕ will be discussed in Sec. 6. There are no regular string solutions at $\varepsilon > 0$.

In Fig. 1, the black line $\varepsilon_*(\Gamma)$ is the upper boundary of the area of class A1 solutions with $r \rightarrow \infty$ as $l \rightarrow \infty$. The points on the black line itself and in the whole area $-1 > \varepsilon \geq \varepsilon_*(\Gamma)$ correspond to class B2 solutions. Fine-tuned solutions with two symmetric regular centers (see Fig. 7) are located along the blue line. The class of fine-tuned solutions with a horizon (B1) is represented by the red line.

Let us briefly describe the classes of solutions presented in the map, postponing the derivation of some important details of the curves to the subsequent sections.

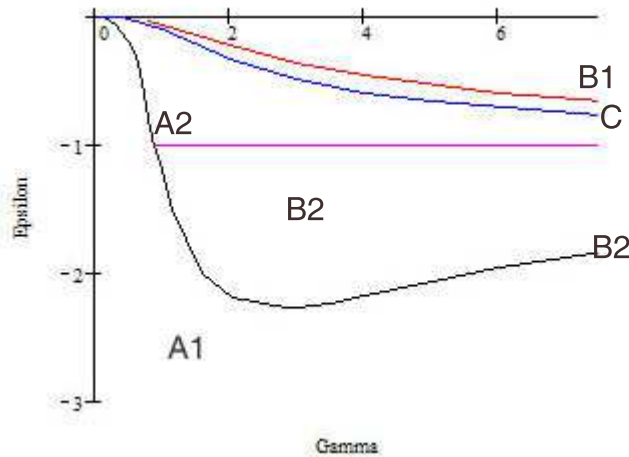


Figure 1: Location of solutions in the plane of parameters (Γ, ε) . The black line $\varepsilon_*(\Gamma)$ is the upper boundary of the area of class A1 solutions with $r \rightarrow \infty$ as $l \rightarrow \infty$. The black line itself and the whole area $-1 > \varepsilon \geq \varepsilon_*(\Gamma)$ correspond to class B2 solutions with $r(\infty) = \text{const}$. Fine-tuned solutions with two symmetric regular centers (class C) are located along the blue line $\varepsilon_1(\Gamma)$. The class B1 of fine-tuned solutions with a horizon is represented by the red line $\varepsilon_h(\Gamma)$.

A: Configurations with infinite r

From Table 1, one can notice a close similarity between the vacuum solutions A0 (where $\phi \equiv 0$) and A1. In fact, the gravitational field in both cases is mainly governed by the (negative) cosmological constant. In the limiting case $|\varepsilon| \gg 1, \varepsilon < 0$ the role of the symmetry breaking potential $V(\phi)$ is negligible. Then, as follows from (14), γ' is always positive, the warp factor $e^{2\gamma}$ grows, and gravity is attractive towards $l = 0$. These solutions with $r \rightarrow \infty$ at large l exist without any fine tuning.

As $|\varepsilon|$ decreases, the potential $V(\phi)$ becomes more and more important, and at ε approaching some $\varepsilon_*(\Gamma)$ the derivative $r' \rightarrow 0$, so that class A1 solutions pass over to asymptotically cylindrical fine-tuned class B2 solutions.

The main features of class A1 solutions at large l are:

- the scalar field $\phi(l)$ tends to a minimum of $V(\phi)$;
- the quantities $\gamma'(l)$ and $\beta'(l)$ tend to the same finite positive constant, so that $e^{\gamma(l)} \sim r(l)$

grow exponentially.

An example of an A1 solution, found numerically, is presented in Fig. 2.

As to the A2 regime, this is an exceptional solution corresponding to the condition $V(0) = 0$, hence $\varepsilon = -1$. In this case [18] a regular integral curve, starting at $l = 0$ with $\phi = 0$, finishes again with $\phi \rightarrow 0$ as $l \rightarrow \infty$. The large l behavior of r and the warp factor $e^{2\gamma}$ in the resulting regular solutions is

$$r \approx l, \quad e^{d_0\gamma} \sim l.$$

B: Asymptotically cylindrical configurations

For these “tube” solutions, it is easy to verify that Eqs. (29)–(31) hold at large l and, in particular, $f \rightarrow f_* = \text{const}$ where $0 < f_*^2 < 1$.

The vacuum solution B0, with $r \equiv r_*$, actually interpolates between the cylindrical asymptotics of B1 ($e^\gamma \rightarrow 0$, a double horizon) and B2 ($e^\gamma \rightarrow \infty$ at $l \rightarrow \infty$, i.e., gravitational attraction towards the center $l = 0$).

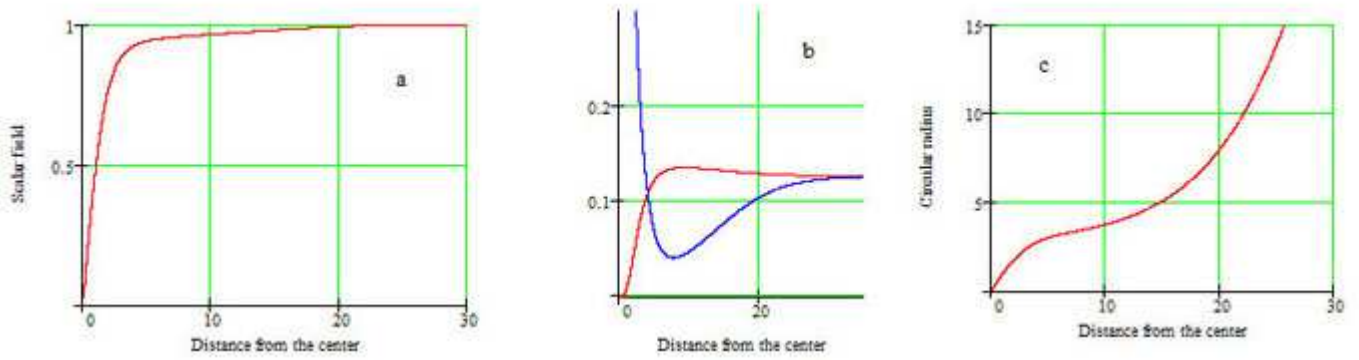


Figure 2: A1 solution with the parameters: $\Gamma = 0.7$, $\varepsilon = -0.9$. (a) — scalar field, (b, blue) — $\beta'(l)$, (b, red) — $\gamma'(l)$, (c) — $r(l)$.

Eq. (31) does not contain \varkappa and allows finding the range of the input parameter ε for which “tube” solutions are possible. The dependence $\varepsilon(f_*)$ is shown in Fig. 3. By Eq. (31),

$$\varepsilon > \varepsilon_{\min} = -1 - \frac{(d_0 - 1)^2}{2d_0 - 1} \quad (33)$$

For $d_0 = 4$, $\varepsilon_{\min} = -16/7 = -2.2857\dots$

It also follows from (31) and Fig. 3 that in the range $-1 > \varepsilon > \varepsilon_{\min}$ there are two branches of the inverse function $f_*(\varepsilon)$. In the range $0 \geq \varepsilon > -1$ there is only one branch. Other limiting values are expressed in terms of f_* by (29)–(32), and

$$\gamma' \rightarrow \varkappa \eta \sqrt{d_0 f_*^2 (1 - f_*^2)}. \quad (34)$$

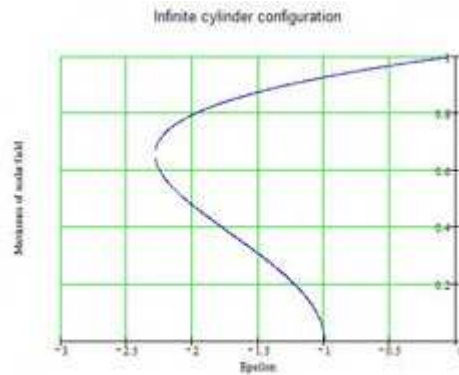


Figure 3: The dependence $\varepsilon(f_*)$ (31) in the infinite cylinder case

Type B2 configurations occupy a whole area in the (ε, Γ) parameter plane, whereas B1 solutions require fine tuning and are located on the red line in the map.

C: Configurations with two centers

As was argued above, type C solutions can be symmetric and asymmetric with respect to reflections $l \rightarrow l_c - l$. Symmetric solutions require one fine-tuning relation, which corresponds to particular curves in the (ε, Γ) plane. The curve describing solutions with a constant sign of ϕ is presented

in Fig.1 (the blue line). Other symmetric configurations will be discussed below. Asymmetric solutions can only appear at discrete points in the parameter plane, and we will not mention them any more.

5. “Tube” solutions: location in the parameter plane

The upper boundary $\varepsilon_*(\Gamma)$ of type A solutions, found numerically point by point for $d_0 = 4$, is presented in Fig.4 by the red line and the circles. Any point in the area $\varepsilon < \varepsilon_*(\Gamma)$, $0 < \Gamma < \infty$ corresponds to a type A solution with f monotonically growing from zero at the center to unity. The function $\varepsilon_*(\Gamma)$ decreases from zero at $\Gamma = 0$ to a minimum with $\varepsilon = \varepsilon_{\min}$ according to Eq. (33) and then grows tending to -1 as $\Gamma \rightarrow \infty$.

In the range $0 > \varepsilon > -1$, the “tube” (fine-tuned) solutions exist only precisely on the line $\varepsilon_*(\Gamma)$, which comprises a border between A and C type solutions.

In the range $-1 > \varepsilon > \varepsilon_*(\Gamma)$, there are cylindrical solutions without fine tuning. This area is located between the zones of A and C type solutions.

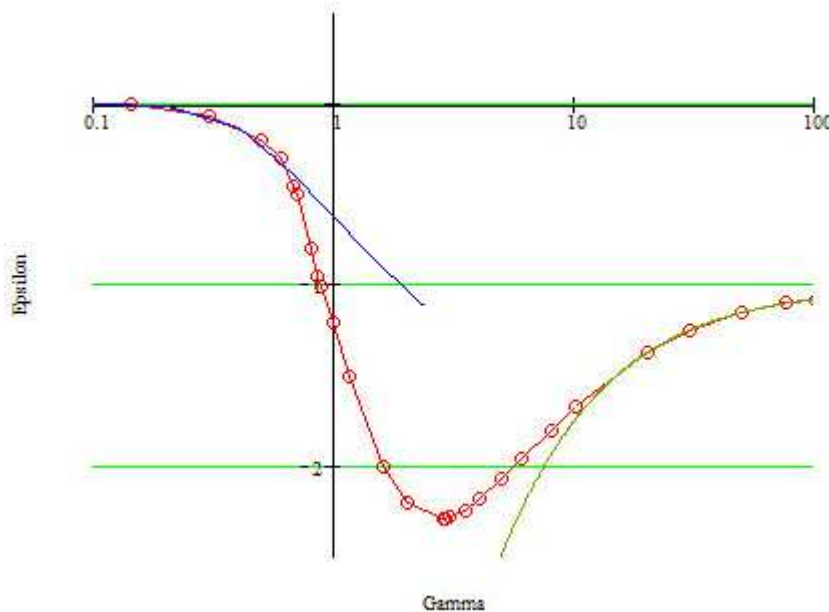


Figure 4: The upper boundary $\varepsilon_*(\Gamma)$ of class A1 solutions with infinite r . The points forming the red line are found numerically. The asymptotic dependences for $\Gamma \ll 1$ (49) and $\Gamma \gg 1$ (40) are shown by the blue and brown curves, respectively.

In the limits of weak and strong gravitational fields (small and large Γ , respectively), a numerical analysis of the field equations is hindered, and we have derived the function $\varepsilon_*(\Gamma)$ analytically. The blue line in Fig. 4 corresponds to $\Gamma \ll 1$, the brown one to $\Gamma \gg 1$.

5.1. Strong gravity: $\Gamma \gg 1$

As follows from numerical analysis, the scalar field in “tube” solutions is small in this case, and the potential can be expanded in a series: $V(\phi) \approx V_0 + \frac{1}{2}V_0''\phi^2$, $dV/d\phi \approx V_0''\phi$. The problem is completely determined by the two constants $V_0 = V(0)$ and $V_0'' = (d^2V/d\phi^2)_{\phi=0}$. Let us introduce a new parameter λ and a new function ψ :

$$\lambda = 4\kappa^2 V_0, \quad \psi = \kappa\phi. \quad (35)$$

For the Mexican hat potential (17), $V_0 = \eta^2(\varepsilon + 1)/4$ and $V_0'' = -1$, so that

$$\lambda = \Gamma(\varepsilon + 1) \quad (36)$$

(recall that $\Gamma := \varkappa^2 \eta^2$). Eqs. (13)–(15) take the form

$$\gamma'' + \gamma'(d_0 \gamma' + \beta') = -\lambda/(2d_0) + \psi^2/d_0, \quad (37)$$

$$\beta'' + \beta'(d_0 \gamma' + \beta') = \psi^2(1/d_0 - e^{-2\beta}) - \lambda/(2d_0), \quad (38)$$

$$\psi'' + \psi'(d_0 \gamma' + \beta') = \psi(e^{-2\beta} - 1) \quad (39)$$

and depend on only one dimensionless parameter λ . The boundary conditions are

$$\gamma(0) = \gamma'(0) = \psi(0) = 0, \quad (e^\beta)'|_{l=0} = 1, \quad \beta'(\infty) = \psi'(\infty) = 0.$$

The scalar field equation (39) is homogeneous with respect to ψ and looks linear; however, the system as a whole is nonlinear, and we have a nonlinear eigenvalue problem. The parameter d_0 being fixed, there is only one dimensionless parameter λ , whose ground state eigenvalue is expected to be of the order of unity. Then according to (36) for $\Gamma \gg 1$, the parameter ε is very close to -1 , and f_0 in (31) is $\sim \Gamma^{-1} \ll 1$. From (39) it follows that $r \equiv e^\beta \rightarrow 1$ at large l . Nontrivial solutions exist for discrete values of λ , one of which, corresponding to a monotonically growing $\psi(l)$, is found numerically:

$$\lambda = -7.433\dots, \quad d_0 = 4.$$

The asymptotic dependence $\varepsilon_*(\Gamma)$ for $\Gamma \gg 1$

$$\varepsilon = -1 + \lambda/\Gamma, \quad \Gamma \gg 1 \quad (40)$$

is presented in Fig. 4 by the brown curve.

5.2. Weak gravity: $\Gamma \ll 1$

The case $\Gamma \ll 1$ is more complicated. A numerical computation shows (and it is verified analytically) that $|\varepsilon|$ is exponentially small as $\Gamma \rightarrow 0$. From (31) we see that $1 - f_0^2 \approx -\varepsilon/(2d_0) \ll 1$, and the limiting value of the circular radius (30), $r_* \approx \sqrt{2d_0/|\varepsilon|}$ is very large as compared with the “core” radius ~ 1 . The equations simplify differently in the two cases $r \ll r_*$ and $r \gg 1$. The solutions should coincide in the intermediate region $1 \ll r \ll r_*$.

It is convenient, for $\Gamma \ll 1$, to rewrite the field equations in terms of $r = e^\beta$:

$$\gamma'' = -\gamma' \left(d_0 \gamma' - \frac{r'}{r} \right) - \frac{\Gamma}{2d_0} [\varepsilon + (1 - f^2)^2], \quad (41)$$

$$r'' = \frac{(d_0 - 1)d_0}{2} \gamma'^2 r - \frac{\Gamma f^2}{2} \frac{f^2}{r} - \frac{\Gamma}{2} f'^2 r - \frac{\Gamma}{4} [\varepsilon + (1 - f^2)^2] r, \quad (42)$$

$$f'' = -f' \left(d_0 \gamma' - \frac{r'}{r} \right) + \frac{f}{r^2} - f(1 - f^2). \quad (43)$$

For $r \ll r_*$ we see that $\gamma' \sim \Gamma \ll 1$, and the term with γ'^2 in (42) can be neglected. In the vicinity of the center, in the terms $\sim \Gamma$, we can set $r = l$ and omit ε . Then Eq. (42) reduces to

$$r'' = -\Gamma \frac{f_0^2}{l} - \frac{\Gamma}{2d_0} (1 - f_0^2)^2 l, \quad \Gamma \ll 1, \quad l \ll r_*,$$

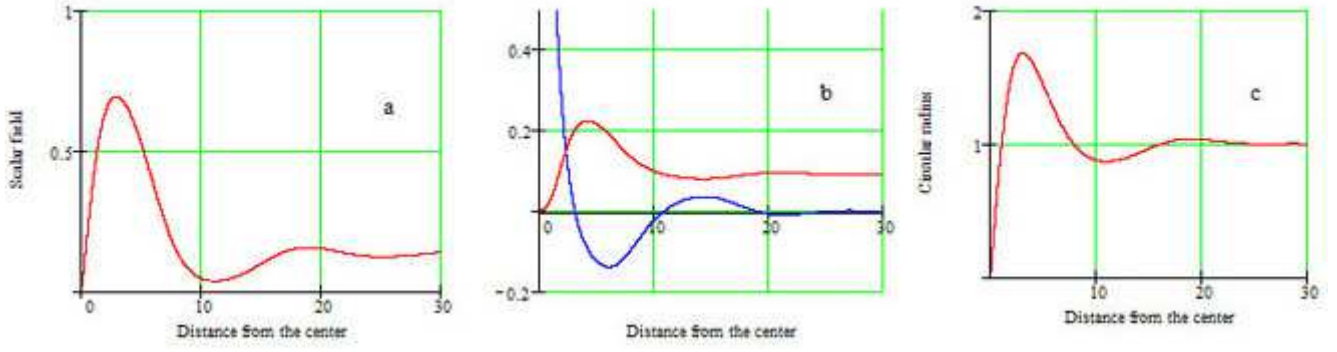


Figure 5: Example of a type B2 solution for $\Gamma = 2$ and $\varepsilon = -1.1$. (a) shows the scalar field $f(l)$, (b) depicts $\gamma'(l)$ and $\beta'(l)$ by the red and blue curves, respectively, and (c) displays $r(l)$.

where f_0 is the solution of (43) with $\gamma' = 0$, $r = l$, and the boundary conditions $f(0) = 0$, $f(\infty) = 1$. With $r'(0) = 1$, after integration we get

$$r' = 1 + \Gamma \left[-f_0^2 \ln l + 2 \int_0^l dl f_0 f_0' \ln l - \frac{1}{2d_0} \int_0^l dl (1 - f_0^2)^2 l \right].$$

The integrals quickly converge for $l \gg 1$, and in the intermediate region $1 \ll l \ll r_*$ we have

$$r'^2 = 1 + 2\Gamma \left(-\ln r + 2J_2 - \frac{J_1}{2d_0} \right), \quad \Gamma \ll 1, \quad 1 \ll r \ll r_*, \quad (44)$$

where the integrals J_1 and J_2 are found numerically:

$$J_1 = \int_0^\infty l dl (1 - f_0^2)^2 = 1, \quad J_2 = \int_0^\infty dl f_0 f_0' \ln l \cong 0.2. \quad (45)$$

In the region $r \gg 1$, Eq. (42) reduces to

$$r'' = -\Gamma \left(\frac{1}{r} + \frac{\varepsilon}{2d_0} r \right), \quad \Gamma \ll 1, \quad 1 \ll r. \quad (46)$$

Taking into account that $r' = 0$ at $r = r_*$, we find

$$\frac{1}{2} r'^2 = \Gamma \left(\ln r_* - \ln r + \frac{\varepsilon}{4d_0} r_*^2 - \frac{\varepsilon}{4d_0} r^2 \right), \quad \Gamma \ll 1, \quad 1 \ll r. \quad (47)$$

In the intermediate region $1 \ll r \ll r_*$ we have

$$r'^2 = 2\Gamma \left(\frac{1}{2} \ln \frac{2d_0}{|\varepsilon} - \ln r - \frac{1}{2} \right), \quad \Gamma \ll 1, \quad 1 \ll r \ll r_*. \quad (48)$$

We have taken into account that $r_* = \sqrt{2d_0/|\varepsilon|}$.

Comparing (44) with (48), we find the fine-tuning relation between ε and Γ for asymptotically cylindrical configurations in the weak gravity limit:

$$\begin{aligned} \varepsilon &= -2d_0 \exp \left(-\frac{1}{\Gamma} - 4J_2 - 1 - \frac{J_1}{d_0} \right) \cong -0.33 d_0 \exp \left(-\frac{1}{\Gamma} + \frac{1}{d_0} \right), \\ \varepsilon &\cong -1.7 e^{-1/\Gamma}, \quad d_0 = 4, \quad \Gamma \ll 1. \end{aligned} \quad (49)$$

This asymptotic dependence $\varepsilon_*(\Gamma)$ for $\Gamma \ll 1$ is presented in Fig. 4 by the blue curve.

5.3. Solutions in the range $-1 > \varepsilon > \varepsilon_*(\Gamma)$

In the range $-1 > \varepsilon > \varepsilon_*(\Gamma)$, there exist type B2 solutions ($r \rightarrow r_* < \infty$ as $l \rightarrow \infty$) without any fine-tuning relation between the parameters ε and Γ . The asymptotic values of the scalar field (f_*) and the radius (r_*) at large l do not depend on Γ :

$$f_*^2 = \frac{d_0 - 1 - \sqrt{(d_0 - 1)^2 + (\varepsilon + 1)(2d_0 - 1)}}{2d_0 - 1},$$

$$r_*^2 = \frac{2d_0 - 1}{d_0 + \sqrt{(d_0 - 1)^2 + (\varepsilon + 1)(2d_0 - 1)}},$$

An example of such a solution is shown in Fig. 5 for $\Gamma = 2$ and $\varepsilon = -1.1$. The scalar field $f(l)$ is shown in Fig. 5a, $\gamma'(l)$ and $\beta'(l)$ are red and blue curves in Fig. 5b, and $r(l)$ is displayed in Fig. 5c.

5.4. Solutions with a horizon

As to type B1 configurations with a horizon, in which $\gamma(l)$ linearly decreases as $l \rightarrow \infty$, their location, found numerically, is shown in Fig. 1 by the red line $\varepsilon = \varepsilon_h(\Gamma)$, corresponding to a certain fine-tuning relation. An example of such a regular solution, with the parameters $\Gamma = 2$, $\varepsilon = -0.233846$, is presented in Fig. 6.

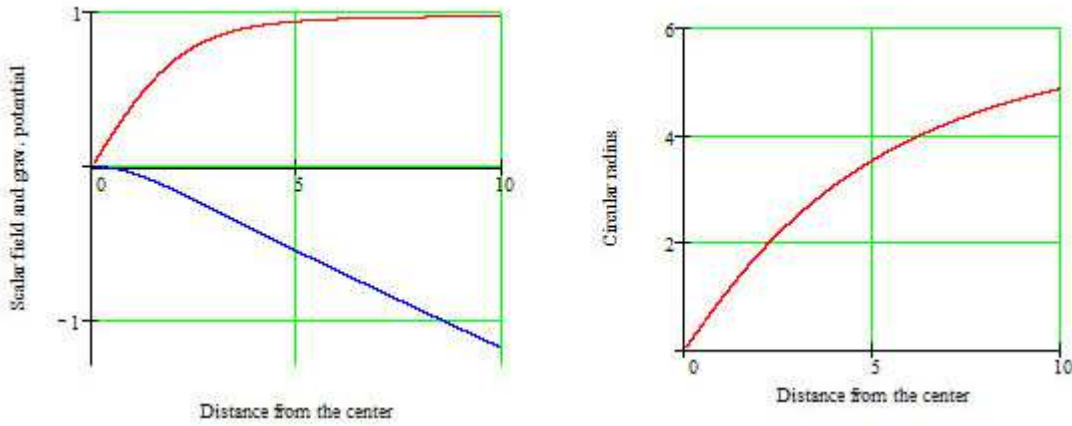


Figure 6: A type B1 solution with a horizon for $\Gamma = 2$ and $\varepsilon = -0.233846$. Left: the scalar field ϕ (red) and the metric function γ (blue). Right: the circular radius r .

The near-horizon metric has the asymptotic form

$$ds^2 = C^2 e^{-2hl} \eta_{\mu\nu} dx^\mu dx^\nu - dl^2 - r_*^2 d\Omega^2, \quad h = \gamma'(\infty). \quad (50)$$

The substitution $e^{-hl} = \rho$ (converting $l = \infty$ to a finite coordinate value, $\rho = 0$) brings the metric (50) to the form

$$ds^2 = C^2 \rho^2 \eta_{\mu\nu} dx^\mu dx^\nu - \frac{d\rho^2}{k^2 \rho^2} - r_*^2 d\Omega^2, \quad \rho \rightarrow 0. \quad (51)$$

Thus $\rho = 0$ is a second-order Killing horizon in the 2-dimensional subspace parameterized by t and ρ ; the extra-dimensional circular radius squared remains positive. It is of the same nature as, e.g., the extreme Reissner-Nordström black hole horizon, or the anti-de Sitter horizon in the second

Randall-Sundrum brane world model. A peculiarity of the present horizon is that the spatial part of the metric, which at large l takes the form $\rho^2(d\vec{x})^2$, is *degenerate* at $\rho = 0$. The volume of the d_0 -dimensional spacetime vanishes as $l \rightarrow \infty$. And it will remain degenerate even if we pass to Kruskal-like coordinates in the (t, ρ) subspace. But the D -dimensional curvature is finite there, indicating that a transition to negative values of ρ (where the old coordinate l no longer works) is meaningful.

Thus solutions with strings (and/or monopoles) in extra dimensions may contain second-order horizons, and the degenerate nature of the spatial metric at the horizon does not lead to a curvature singularity; moreover, the metric may be continued in a Kruskal-like manner. However, the zero volume of the spatial section makes the density of any additional (test) matter infinite at $\rho = 0$. To consider these solutions as describing viable configurations, one needs to take into account the back-reaction of ordinary matter. It will evidently destroy such a configuration.

6. Solutions with two regular centers: location in the parameter plane

Symmetric type C solutions with two regular centers are located on the (ε, Γ) plane in the region $0 > \varepsilon > -1$ to the right from the **red** fine-tuning curve $\varepsilon_*(\Gamma)$ in Fig. 4 or, which is the same, to the right of the black line in the full map, Fig. 1. The solutions are fine-tuned, i.e., located along certain lines $\varepsilon_N(\Gamma)$ in this region, where N is the number of half-waves, $N - 1$ is the number of knots (zeros) of the scalar field $f = \phi/\eta$. The point is that f , just as the radius r , is zero at both centers, but f can change its sign. So there are several families of regular solutions with different numbers N of half-waves, each family corresponding to a line $\varepsilon_N(\Lambda)$ in the parameter plane. The blue curve in Fig. 1 depicts $\varepsilon_1(\Lambda)$.

6.1. Solutions without knots of the scalar field

In solutions where f has a constant sign, all three functions $f(l)$, $r(l)$ and $\gamma(l)$ reach their extremum values at the equator $l = l_{\text{eq}}$. Setting in the first integral (16)

$$f'(l_{\text{eq}}) = r'(l_{\text{eq}}) = \gamma'(l_{\text{eq}}) = 0, \quad (52)$$

we find a relation between $f(l_{\text{eq}}) =: f_{\text{eq}}$ and $r(l_{\text{eq}}) =: r_{\text{eq}}$:

$$r_{\text{eq}}^2 = \frac{2f_{\text{eq}}^2}{|\varepsilon| - (1 - f_{\text{eq}}^2)^2}. \quad (53)$$

It is convenient to use (53) together with (52) as boundary conditions and perform numerical integration from the equator to one of the centers. Then the three conditions $f(l_c) = 0$, $r(l_c) = 0$ and $r'(l_c) = 1$ determine the values of f_{eq} and l_c and a fine-tuning relation $\varepsilon = \varepsilon_1(\Gamma)$.

An example of a configuration with two regular centers is presented in Fig. 7 for $\Gamma = 2$; the fine-tuned value of ε is $\varepsilon_1(2) = -0.3326\dots$, it belongs to the line $\varepsilon = \varepsilon_1(\Gamma)$.

The (blue) curve $\varepsilon = \varepsilon_1(\Gamma)$ in Fig. 1 has been obtained numerically. For small and large values of Γ , this fine-tuning relation can be derived analytically.

$\varepsilon_1(\Gamma)$ **for weak gravity**, $\Gamma \ll 1$

This derivation repeats the one for Eq. (49). The main difference is that now we get from (53) the value of $r(l)$ at the equator

$$r_{\text{eq}} = r(l_{\text{eq}}) = \sqrt{2/|\varepsilon|}, \quad |\varepsilon| \ll 1 \quad (54)$$

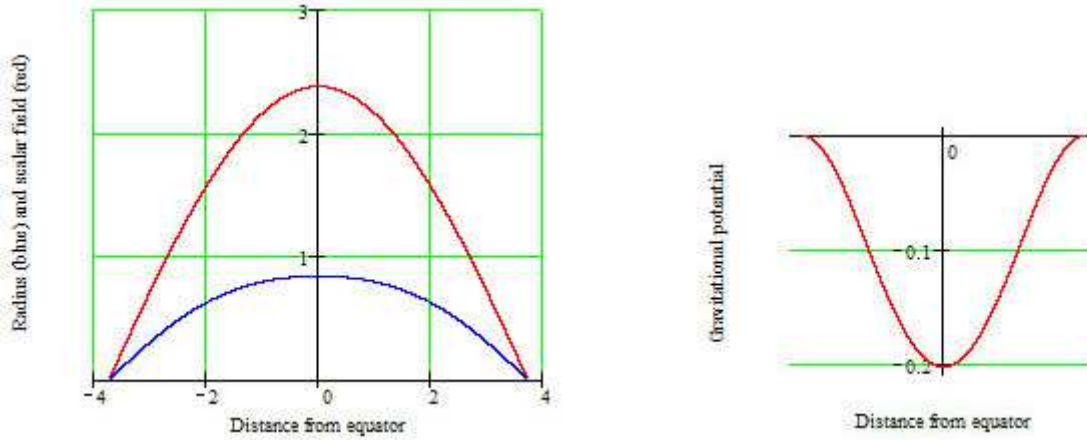


Figure 7: Example of a configuration with two symmetric regular centers without knots of the scalar field. $\Gamma = 2$, the fine-tuned value $\varepsilon_1(2) = -0.3326\dots$. It belongs to the line $\varepsilon = \varepsilon_1(\Gamma)$. Left: $r(l)$ — red, $f(l)$ — blue; right: $\gamma(l)$.

and use it instead of r_* . Substituting (54) into (47), we have instead of (48)

$$r'^2 = \Gamma \left(\ln \frac{2}{|\varepsilon|} - 2 \ln r - \frac{1}{d_0} - \frac{\varepsilon}{2d_0} r^2 \right), \quad \Gamma \ll 1, \quad 1 \ll r.$$

In the intermediate region $1 \ll r \ll r_m$ it should coincide with (44). The resulting relation is

$$\varepsilon = -2 \exp \left(-\frac{1}{\Gamma} - \frac{1 - J_1}{d_0} - 4J_2 \right) \cong -0.9 e^{-1/\Gamma}, \quad \Gamma \ll 1. \quad (55)$$

$\varepsilon_1(\Gamma)$ **for strong gravity**, $\Gamma \gg 1$

Numerical integration shows that for $\Gamma \gg 1$ the scalar field f remains small in the whole interval between the centers, while $\psi = \varkappa \eta f$ is of the order of unity. Introducing, as before, λ (36) and taking into account that $f \ll 1$, we again find Eqs. (37)–(39). It is convenient to integrate them from the equator to a center and to use boundary conditions in the form

$$\beta'(l_{\text{eq}}) = \psi'(l_{\text{eq}}) = \gamma'(l_{\text{eq}}) = 0, \quad \psi(l_{\text{eq}}) = \psi_{\text{eq}}, \quad \beta(l_{\text{eq}}) = \frac{1}{2} \ln \frac{2\psi_{\text{eq}}^2}{2\psi_{\text{eq}}^2 - \lambda}. \quad (56)$$

The three parameters ψ_{eq} , $l_c - l_{\text{eq}}$ and λ should be determined from the conditions

$$\psi(l_c) = 0, \quad r(l_c) = 0, \quad r'(l_c) = 1.$$

Numerical integration results in $\lambda = 1.9\dots$

Thus, for type C solutions, the desired fine-tuning relation in the strong gravity limit is

$$\varepsilon = -1 + 1.9/\Gamma. \quad (57)$$

6.2. Odd and even scalar fields

In the above solutions, the scalar field $f(l)$ without knots is an even function.

Since $f(l)$ may change its sign between the centers, there are two possibilities. If the number of knots of $f(l)$ is even, then $f(l)$ is an even function, reaching an extremum at the equator, and $f'(l_{\text{eq}}) = 0$. On the contrary, $f(l)$ with an odd number of knots is an odd function: $f(l_{\text{eq}}) = 0$, and $f'(l)$ is then an even function having an extremum at $l = l_{\text{eq}}$.

Numerical integration of Eqs. (13)–(15) in the case of an even number of knots can be performed with the same boundary conditions (56) as without knots. The results are displayed in Figs. 8–10.

Fig. 8 shows a few solutions for the scalar field $f(l)$ with 2 knots and the corresponding functions $r(l)$.

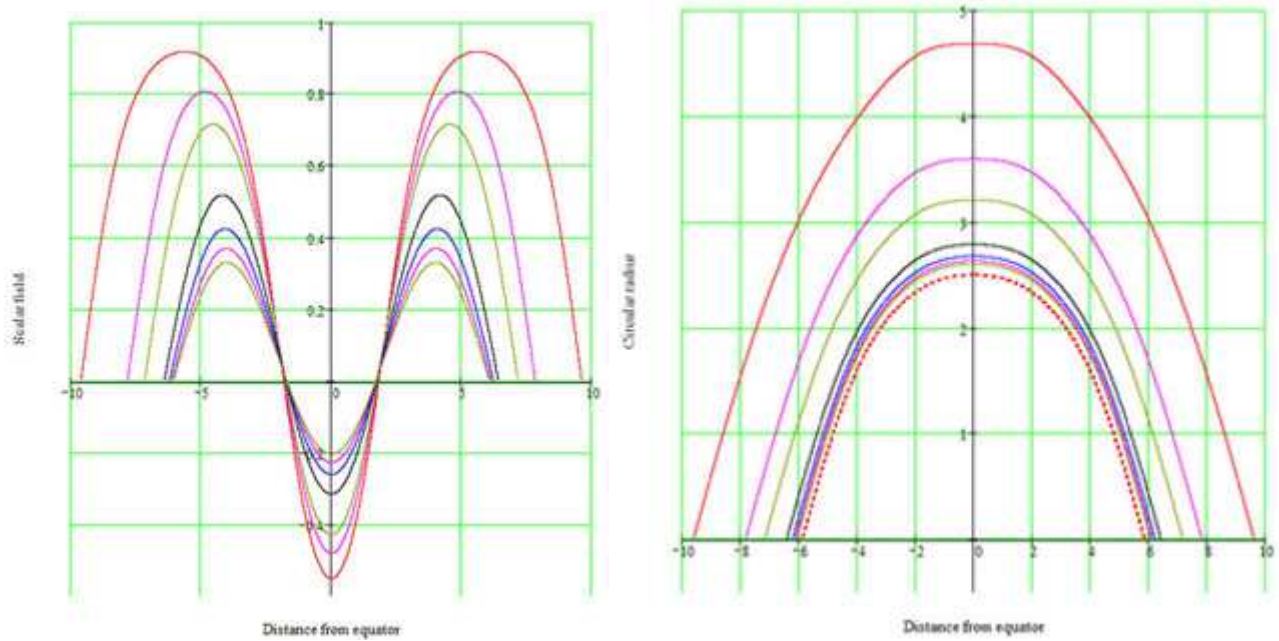


Figure 8: Solutions with two symmetric regular centers with 2 knots of $f(l)$ for $\Gamma = 0.5, 0.75, 1, 2, 3, 4$ and 5 in the order of decreasing amplitude. The corresponding fine-tuned values of ε are $-0.51275, -0.62765, -0.7019, -0.8365, -0.888, -0.9146,$ and -0.93115 . Left: $f(l)$. Right: $r(l)$; the additional dashed curve corresponds to the limit $\Gamma \rightarrow \infty$.

Fig. 9 shows the function $\gamma(l)$ in the whole range of l and (b) in a close vicinity of the equator for visual clarity, to demonstrate a minimum at the equator. Recall that γ enters into the equations only via γ' and γ'' , and so, without loss of generality, we have put $\gamma(l_{\text{eq}}) = 0$ in Fig. 9 (b). The larger is Γ , the deeper is the local minimum of γ at the equator. Altogether, the gravitational potential has three minima: one at the equator and two others near the regular centers.

The fine-tuning relation $\varepsilon_3(\Gamma)$ for solutions with two knots of $f(l)$, found numerically, is shown in Fig. 10. Each curve in Figs. 8 and 9 corresponds to a point on this curve.

In solutions with an odd number of knots of $f(l)$, we have $f(l_{\text{eq}}) = 0$, and from (16) we obtain at the equator $f'^2 = (\varepsilon + 1)/2$. For numerical integration of Eqs. (13)–(15) in this case, it is convenient to use the following boundary conditions:

$$\beta'(l_{\text{eq}}) = f(l_{\text{eq}}) = \gamma'(l_{\text{eq}}) = 0, \quad \beta(l_{\text{eq}}) = \beta_{\text{eq}}, \quad f'(l_{\text{eq}}) = \sqrt{(\varepsilon + 1)/2}. \quad (58)$$

Then the three conditions $f(l_c) = 0$, $r(l_c) = 0$ and $r'(l_c) = 1$ determine the values of β_{eq} and $l_c - l_{\text{eq}}$ as well as the fine-tuning relation ($\varepsilon = \varepsilon_2(\Gamma)$ in the case of one knot). As an example, in

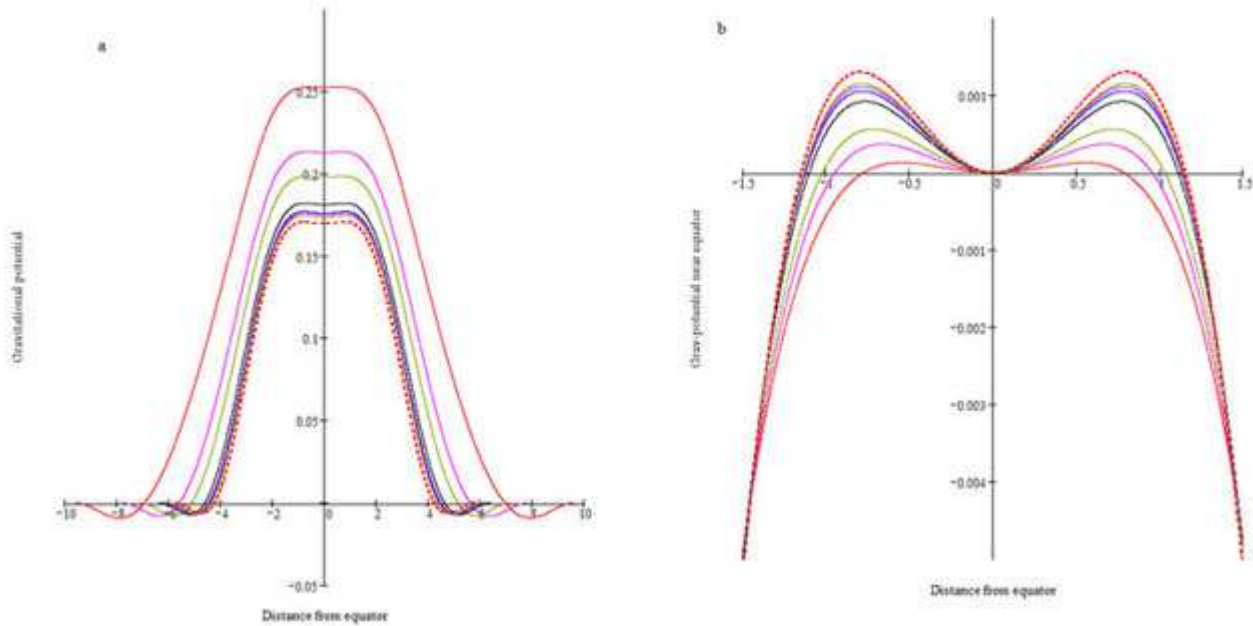


Figure 9: The functions $\gamma(l)$ (a) in the whole range of l and (b) in a close vicinity of the equator for the solutions with the same set of parameters as in Fig. 8.

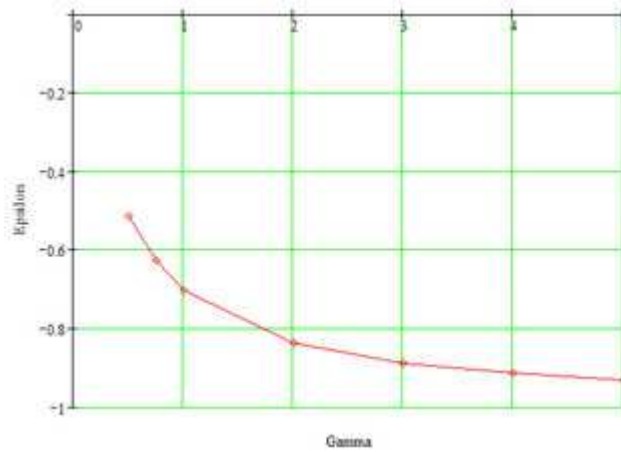


Figure 10: The fine-tuning relation $\varepsilon_3(\Gamma)$ for solutions with two knots of $f(l)$ between the centers, displayed in Figs. 8 and 9.

Fig. 11 we present a numerical solution with one knot for $\Gamma = 2$, corresponding to $\varepsilon = -0.71$. The left graph shows $r(l)$ (red) and $f(l)$ (blue). $\gamma(l)$ is depicted on the right graph. The function $\gamma(l)$ is symmetric relative to the equator and has two minima close to the centers.

One can note that if we include into consideration configurations with angular deficits and excesses at the centers, then the existence of solutions with two centers is not restricted to particular lines in the (ε, Γ) plane. There will be a whole area of such solutions, bounded by $\varepsilon = \min(\varepsilon_*(\Gamma), -1)$ from below, and by the line $\varepsilon = \varepsilon_h(\Gamma)$ from above. Among the nonsymmetric solutions of this kind with several knots of the scalar field one can find those with multiple local maxima and minima of $\gamma(l)$. Their possible connection with matter trapping and the hierarchy problem is discussed below.

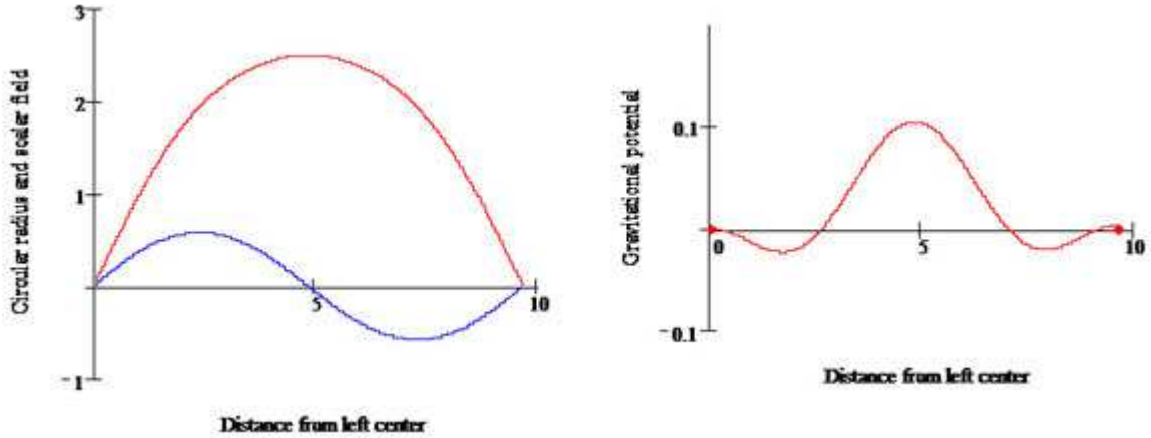


Figure 11: Example of a solutions with two symmetric regular centers and an odd scalar field with one knot. $\Gamma = 2$, the corresponding fine-tuned value $\varepsilon_2(\Gamma) = -0.71$. The left graph shows $r(l)$ (red) and $f(l)$ (blue); $\gamma(l)$ is depicted on the right graph.

7. Matter in the background of global string configurations

In this section we discuss the problem of trapping of classical point particles and test scalar fields by the gravitational field of the global string configurations described above.

7.1. Classical particles

The motion of classical particles in the bulk may be equivalently described in terms of geodesics or using the Hamilton-Jacobi equation. We here use the second approach.

The Hamilton-Jacobi equation for a point test particle of (primary) mass m_0 in space-time with the metric (10) is

$$e^{-2\gamma(l)} \left[\left(\frac{\partial S}{\partial t} \right)^2 - \left(\frac{\partial S}{\partial \vec{x}} \right)^2 \right] - \left(\frac{\partial S}{\partial l} \right)^2 - \frac{1}{r^2(l)} \left(\frac{\partial S}{\partial \theta} \right)^2 - m_0^2 = 0,$$

The metric is homogeneous with respect to all coordinates except l , and the action can be written in the form

$$S = Et - \vec{p}\vec{x} + S_l(l) + M\theta, \quad (59)$$

where E is the particle energy, \vec{p} is the particle momentum along the coordinates x^i , $i = \overline{1, d_0 - 1}$, θ is the angular coordinate in the extra dimensions (note that $d\Omega^2 = d\theta^2$ for $d_1 = 1$) and M is its conjugate angular momentum. The remaining unknown function $S_l(l)$ satisfies the equation

$$\frac{dS_l}{dl} = \pm \sqrt{p^2 e^{-2\gamma(l)} - \frac{M^2}{r^2(l)} - m_0^2},$$

where $p^2 = E^2 - \vec{p}^2$. Zeros of the square root determine the turning points of classical motion.

Consider a particle with $M = 0$, i.e., moving in the bulk along the coordinate l (strictly to or from a brane if the latter is located at fixed l). Classical motion is allowed where the square root is real. The turning points l_t are determined by the equation

$$p^2 e^{-2\gamma(l_t)} - m_0^2 = 0.$$

If there is a minimum of $\gamma(l)$ at some $l = l_0$, a classical particle with $p^2 = m_0^2 e^{2\gamma(l_0)}$ cannot move along the l direction and is trapped precisely at this minimum of γ . Particles with slightly larger p^2 can move between two turning points in the vicinity of l_0 . If it is a global minimum of γ , particles with any $p^2 \geq m_0^2 e^{2\gamma(l_0)}$ are trapped.

It can also be verified that particles with the same value of p^2 but $M \neq 0$ (moving in the θ direction) have a still more narrow range of motion along l .

In particular, near the equator of a configuration with two centers and three half-waves of ϕ (see Fig. 9), the turning points of finite classical motion exist for $\gamma(l_{\text{eq}}) < \gamma < \gamma_m$, where γ_m is the maximum of $\gamma(l)$. Denoting $m_{\text{eq}}^2 = m_0^2 e^{2\gamma(l_{\text{eq}})}$, we see that a classical particle is trapped near the equator if its energy is restricted by

$$m_{\text{eq}}^2 < p^2 < m_{\text{eq}}^2 e^{2[\gamma_m - \gamma(l_{\text{eq}})]}.$$

It moves along the Minkowski coordinates as a free particle of mass m_{eq} .

7.2. Scalar fields

Consider a test scalar field χ with the Lagrangian L_χ such that

$$2L_\chi = \partial^A \chi^* \partial_A \chi - m_0^2 \chi^* \chi \quad (60)$$

in the background of our string configurations with the metric (10). Here, the asterisk as a superscript denotes complex conjugation and m_0 is the initial field mass. The χ field obeys the Klein-Gordon equation

$$\partial_A (\sqrt{g} g^{AB} \partial_B \chi) + \sqrt{g} m_0^2 \chi = 0, \quad (61)$$

where $g = |\det(g_{AB})| = e^{2d_0\gamma + 2\beta}$. Taking into account the symmetry of the problem, we can take a single mode of χ , assuming

$$\chi(x^A) = X(l) e^{-ip_\mu x^\mu} e^{in\theta}, \quad (62)$$

where $p_\mu = (E, \vec{p})$ is the ($d_0 = 4$)-momentum along the brane and n is an integer. Then $X(l)$ obeys the equation

$$X'' + (d_0\gamma' + \beta')X' + (p^2 e^{-2\gamma} - n^2 e^{-2\beta} - m_\chi^2)X = 0, \quad (63)$$

where $p^2 = p_\mu p^\mu = E^2 - \vec{p}^2$ is the effective mass squared, observed on the brane.

As a trapping criterion for a mode X , it is reasonable to require finiteness of the χ field energy E_χ per unit area of the brane,

$$E_\chi = \int T_t^t[\chi] \sqrt{g} d\theta dl = 2\pi \int T_t^t[\chi] \sqrt{g} dl < \infty, \quad (64)$$

where

$$T_t^t[\chi] = \frac{1}{2} [e^{-2\gamma}(E^2 + \vec{p}^2) + X'^2 + (n^2 e^{-2\beta} + m_0^2)X^2] \quad (65)$$

is the temporal component of the χ field stress-energy tensor. One can notice that the validity of (64) automatically guarantees finiteness of the norm $\int \sqrt{g} \chi^* \chi dl d\theta$ of the χ field considered as a quantum-mechanical wave function.

The finiteness of E_χ in the background of different regular configurations with infinite extra dimensions described above depends on the behavior of solutions to (63) at small and large l .

We begin with considering the χ field behavior near a regular center $l = 0$, which is common to all classes of regular configurations. At small l , we have $e^\beta \equiv r \sim l$ and $\gamma \rightarrow 0$. Hence Eq. (63) takes the approximate form

$$lX'' + X' + l(p^2 - m_0^2)X = 0 \quad (n = 0), \quad (66)$$

$$lX'' + X' - (n^2/l)X = 0 \quad (n \neq 0). \quad (67)$$

Eq. (66) is solved by zero-order cylindrical functions if $p^2 \neq m_0^2$ and in elementary functions if $p^2 = m^2$; Eq. (67) is an Euler equation. The solutions behave as follows at small l :

$$\begin{aligned} X &\approx C_1 + C_2 \ln l & (n = 0), \\ X &\approx C_3 l^n + C_4 l^{-n} & (n \neq 0), \end{aligned} \quad (68)$$

with integration constants C_i . To make the integral in (64) converge as $l \rightarrow 0$, one should choose $C_2 = 0$ and $C_4 = 0$, i.e., in each case, only one of the two linearly independent solutions.

Now, consider the asymptotic form of solutions to Eq. (63) as $l \rightarrow \infty$ for different background configurations.

A1: at large l , $\gamma \sim \beta \sim hl$, $h = \text{const} > 0$. In Eq. (63), the terms with p^2 and m^2 are negligible, and the solution has the asymptotic form

$$X \approx C_+ e^{-a+l} + C_- e^{-a-l}, \quad 2a_\pm = (D-1)h \pm \sqrt{(D-1)^2 h^2 + 4m_0^2}, \quad (69)$$

where C_\pm are integration constants and $D = d_0 + 2$ is the full space-time dimension. It is easy to verify that the criterion (64) holds for the solution with $C_+ \neq 0$, $C_- = 0$. Thus scalar fields with any nonzero mass can be trapped on such branes.

A2: at large l , $e^{d_0 \gamma} \sim e^\beta \sim l$. Again, the terms with p^2 and m^2 are negligible, and Eq. (63) transforms to $X'' + 2X'/l - m_0^2 X = 0$ whose solution is

$$X \approx (C_+ e^{m_0 l} + C_- e^{-m_0 l})/l, \quad (70)$$

and evidently the solution with $C_+ = 0$ satisfies the criterion (64).

B1: at large l , $r \equiv e^\beta \rightarrow r_*$, $\gamma \approx -hl$, $h > 0$, and the approximate form of Eq. (63) is

$$X'' - d_0 h X' + p^2 e^{2hl} X = 0. \quad (71)$$

For $p \neq 0$, it is solved in cylindrical functions, the general solution being

$$X = e^{d_0 hl/2} Z_{d_0/2} \left(\frac{|p|}{h} e^{hl} \right) \sim e^{(d_0-1)hl/2} \sin \left(\frac{|p|}{h} e^{hl} + \Phi \right), \quad (72)$$

where Φ is a constant phase. It is easy to verify that E_χ diverges as $\int e^{hl} dl$. So massive modes with any $p^2 > 0$ are not trapped by B1 configurations.

B2: at large l , $r \rightarrow r_*$ and $\gamma \approx hl$, $h > 0$. The situation is almost the same as in case A1; the solution to (63) has the asymptotic form (69) with the replacements

$$D-1 \mapsto d_0, \quad m_0^2 \mapsto m_0^2 + n^2/r_*^2.$$

Again, only the solution with $C_- = 0$ provides convergence of E_χ .

Thus the configurations of classes A1, A2 and B2 can trap massive scalar modes; since at both large and small l only one of the two linearly independent solutions to (63) is selected, we have a boundary-value problem with a discrete spectrum of p^2 for any given values of m_0 , n and the background parameters.

7.3. The Schrödinger equation

It is helpful to reformulate the boundary-value problem for scalar field modes in terms of the Schrödinger equation. To do so, we make the following substitutions in (63):

$$dl = e^\gamma dx, \quad X(l) = y(x)/\sqrt{f(x)}, \quad (73)$$

where $f(x) = e^{(d_0-1)\gamma+\beta}$. The new variable x is actually an analogue of the well-known ‘‘tortoise coordinate’’ in the analysis of spherically symmetric metrics, such that the metric takes the form

$$ds^2 = e^{2\gamma}(\eta_{\mu\nu}dx^\mu dx^\nu - dx^2) - e^{2\beta} d\theta^2. \quad (74)$$

Then Eq. (63) transforms to the Schrödinger form

$$y_{xx} + [p^2 - V_{\text{eff}}(x)]y = 0 \quad (75)$$

with the effective potential

$$V_{\text{eff}} = (m_0^2 + n^2 e^{-2\beta}) e^{2\gamma} + \frac{f_{xx}}{2f} - \frac{f_x^2}{4f^2}, \quad (76)$$

where the subscript x denotes d/dx . Recall that the eigenvalue p^2 is the effective mass squared, observed in Minkowski space.

Near the center (without loss of generality, $x \approx l \rightarrow 0$), we have

$$V_{\text{eff}} \approx n^2/x^2 + m_0^2 + \frac{1}{4} \left[1 + 2(d_0 - 1)\gamma_{xx} + \beta_{xx} \right]_{x=0}. \quad (77)$$

So for $n \neq 0$ it is a potential wall whereas $V_{\text{eff}} \rightarrow \text{const}$ for $n = 0$.

At large l for different backgrounds, we have:

$$\begin{aligned} \mathbf{A1} : \quad & x \rightarrow x_+ < \infty; \quad x_+ - x \sim e^{-hl}, \quad h > 0; \\ & V_{\text{eff}}(x) \approx e^{2hl} \left[m_0^2 + \frac{h^2}{4}(d_0^2 + 2d_0) \right]. \end{aligned} \quad (78)$$

$$\begin{aligned} \mathbf{A2} : \quad & x \sim l^{(d_0-1)/d_0} \rightarrow \infty; \\ & V_{\text{eff}}(x) \approx m_0^2 e^{2\gamma} \sim l^{2/d_0} \sim x^{2/(d_0-1)}. \end{aligned} \quad (79)$$

$$\begin{aligned} \mathbf{B1} : \quad & x \sim e^{hl} \rightarrow \infty, \quad h > 0; \\ & V_{\text{eff}}(x) \approx e^{-2hl} \left[m_0^2 + \frac{n^2}{r_*^2} + \frac{h^2}{4}(d_0^2 - 1) \right] \sim \frac{1}{x^2}. \end{aligned} \quad (80)$$

$$\begin{aligned} \mathbf{B2} : \quad & x \rightarrow x_* < \infty; \quad x_* - x \sim e^{-hl}, \quad h > 0; \\ & V_{\text{eff}}(x) \approx e^{2hl} \left[m_0^2 + \frac{n^2}{r_*^2} + \frac{h^2}{4}(d_0^2 - 1) \right]. \end{aligned} \quad (81)$$

We see that in the cases A1, A2, B2 the potential is rising to infinity at large l , which leads to discrete spectra of p^2 . For B1 configurations (with a horizon at $l = \infty$), in usual quantum mechanics we would expect a continuous spectrum of states; in our case, with the appropriate boundary conditions, as we saw above, there are no admissible states with $p^2 > 0$.

7.4. Massless modes in configurations with infinite extra dimensions

For a possible massless mode, $p^2 = m_0^2 = n^2 = 0$, Eq. (63) is easily solved:

$$X' = C_1 e^{-d_0\gamma-\beta}, \quad X = C_1 \int e^{-d_0\gamma-\beta} dl + C_2, \quad C_{1,2} = \text{const.} \quad (82)$$

and X is found by quadrature.

One of the solutions is $X = \text{const.}$ It is easy to verify that with this solution, which is well-behaved at a regular center, the energy E_χ (64) diverges at large l in the backgrounds A1, A2, B2 but converges in the background B1.

For the other solution with $C_1 \neq 0$, on the contrary, E_χ converges at large l in the backgrounds A1, A2 and B2 and diverges in B1. This solution, however, is singular at the center and leads there to a divergence in E_χ .

Thus B1 configurations with horizons, being unable to trap massive scalar fields, are the only ones that can trap a massless scalar.

8. Configurations with two centers and the hierarchy problem

In configurations with two symmetric regular centers and two knots of the scalar field, there are three minima of the “gravitational potential” γ , see Fig. 9. The minimum at the equator is higher than the other two, located near the centers. A similar (and even more complicated) structure may be expected for configurations with a larger number of scalar field knots. The minima of γ are able to trap classical particles. As to quantum ones (at least for zero spin), the effective potential (76) not necessarily has a minimum precisely where γ has a minimum, and an additional detailed study is necessary. Though, at least quasiclassically, quantum and classical particles must be trapped in close positions, and the main difference between them is that quantum particles can tunnel from a higher minimum of V_{eff} to a lower one.

Now, suppose a particle described by a certain mode of the χ field (for simplicity, with $n = 0$) is trapped at some position l_i . The mode equation (63) may be rewritten in the form

$$(\sqrt{g}X')' + \sqrt{g}X e^{-2\gamma}p^2 = \sqrt{g}m_0^2X. \quad (83)$$

Let us integrate this equation over the extra dimension from one center to the other. The term $\int (\sqrt{g}X')' dl = 0$ because $\sqrt{g} = r e^{d_0\gamma}$ is zero at both centers. For a particle trapped at some fixed position $l = l_i$, we get

$$p^2 = m_i^2 = m_0^2 \frac{\int \sqrt{g}X dl}{\int \sqrt{g} e^{-2\gamma}X dl} \approx m_0^2 e^{2\gamma(l_i)}. \quad (84)$$

To interpret this result, we note that the whole picture looks quite different depending on the size of the extra dimensions, characterized by the distance l_c between the centers. This size, in turn, varies with the value of $\Gamma = \varkappa^2\eta^2$: it is close to unity (i.e., the length unit which is also arbitrary) for large Γ and tends to infinity as $\Gamma \rightarrow 0$. For (comparatively) weak gravity of the string, $\Gamma \rightarrow 0$, when l_c is very large, all minima of $\gamma(l)$ form individual branes located in the bulk far from one another. In this case, an observer located on one of the branes sees only particles corresponding to modes trapped on this brane; tunnelling from one brane to another will be seen as appearance or disappearance of observable particles. The whole picture may be used for treating the interaction hierarchy problem in the spirit of Randall and Sundrum’s first model [4].

In the opposite case $\Gamma \rightarrow \infty$ (and provided the unit length $(\lambda_0 \eta)^{-1/2}$ is also sufficiently small), l_c can be a length invisible for modern instruments, say, $l_c \ll 10^{-17}$ cm. We then arrive at a picture close to the original Kaluza-Klein concept; particles with the same primary mass m_0 , being trapped at different minima of the effective potential, are seen as particles with different masses, and the tunneling process from a higher minimum to a lower one is observed as a decay of a particle of larger mass to that of smaller mass, with energy release in some form. This may be a natural explanation of the existing families of particles with different masses but similar other properties. A more detailed study of this opportunity is desirable but is beyond the scope of the present paper.

9. Conclusion

Our phenomenological approach based on the macroscopic theory of phase transitions with spontaneous symmetry breaking allows us to study the general physical properties of topological defects in the framework of the brane world concept. In particular, in this paper we have studied the gravitational properties of global strings located in extra dimensions. We have given a general description and classification of possible regular solutions and presented a map showing the location of different solutions in the space of physical parameters.

Among the variety of regular solutions, there are ones possessing brane features, including those with multiple branes, as well as those of potential interest from the viewpoint of the hierarchy problem.

In connection with branes, we have analyzed the possibilities of trapping of classical particles and scalar fields. We have shown that, contrary to a domain wall, in the case of an extra-dimensional global string, matter can be trapped by gravity even without coupling to the scalar field that forms the string itself.

Among the configurations with two centers, the structures having several minima of $\gamma(l)$ may be of interest in connection with the hierarchy problem. If the distance between the centers is small, we work within the Kaluza-Klein concept, and the same particle, being trapped at different minima, looks for an observer as a family of similar particles with different rest masses.

Acknowledgement

We appreciate partial financial support from Russian Basic Research Foundation Project No. 05-02-17478.

References

- [1] T. Kaluza, Sitzungsber. Preuss. Akad. Wiss. Berlin, Math. Phys. **K1**, 966 (1921);
O. Klein, Z. Phys. **37**, 895 (1926).
- [2] K. Akama, Lect. Notes Phys. 176, 267 (1982);
V.A. Rubakov and M.E. Shaposhnikov, Phys. Lett. 125B, 136 (1983);
M. Visser, Phys. Lett. 159B, 22 (1985);
E.J. Squires, Phys. Lett. 167B, 286 (1986);
G.W. Gibbons and D.L. Wiltshire, Nucl. Phys. B 717, (1987).
- [3] P. Horava and E. Witten, Nucl. Phys. B 460, 506 (1996); B475, 94 (1996);
E. Witten, Nucl. Phys. B 471, 135 (1996).
- [4] L. Randall and R. Sundrum, “Large mass hierarchy from a small extra dimension”, *Phys. Rev. Lett.* **83**, 3370-3373 (1999).
- [5] B. Acharya, K. Bobkov, G. Kane, P. Kumar, and D. Vaman, “M theory Solution to the Hierarchy Problem”, hep-th/0606262;
G. Burdman, “New Solutions to the Hierarchy Problem”, hep-ph/0703194;
S. Das, A. Dey and S. SenGupta. “Readdressing the hierarchy problem in a Randall-Sundrum scenario with bulk Kalb-Ramond background”, *Class. Quant. Grav.* **23**, L67-72 (2006); hep-th/0511247;
P. Chen, “Dark energy and the hierarchy problem”, hep-ph/0611378;
S. Das, A. Dey and S. SenGupta, “Randall-Sundrum with Kalb-Ramond field: return of the hierarchy problem?”, gr-qc/0610021;
T. Biswas and A. Notari, “Can inflation solve the hierarchy problem?”, hep-ph/0511207;
G. Cognola, E. Elizalde, S. Nojiri, S.D. Odintsov, and S. Zerbini. “Dark energy in modified Gauss-Bonnet gravity: late-time acceleration and the hierarchy problem”, hep-th/0601008;
S. Das, A. Dey and S. SenGupta, “Stability and hierarchy problems in string inspired brane world scenarios”, hep-th/0704.3113;
C.S. Lim, N. Maru and K. Hasegawa, “Six-dimensional gauge-Higgs unification with an extra space S² and the hierarchy problem”, hep-th/0605180.
- [6] D.A. Kirzhnits, Pis'ma Zh. Eksp. Teor. Fiz. 15, 745 (1972) [*JETP Lett.* 15, 529 (1972)].
- [7] Ya.B. Zel'dovich, I.Yu. Kobzarev, and L.B. Okun', Zh. Eksp. Teor. Fiz. 67, 3 (1974) [*Sov. Phys. JETP* 40, 1 (1975)].
- [8] O. DeWolfe, D.Z. Freedman, S.S. Gubser and A. Karch, “Modeling the fifth dimension with scalars and gravity”, *Phys. Rev. D* **62**, 046008 (2000); hep-th/9909134.
- [9] M. Gremm, *Phys. Rev. D* **62**, 044017 (2000);
A. Davidson and P.D. Mannheim, “Dynamical localizations of gravity”, hep-th/0009064;
C. Csaki, J. Erlich, T.J. Hollowood and Y. Shirman, *Nucl. Phys. B* **581**, 309 (2000);
D. Bazeia, F.A. Brito and J.R. Nascimento, *Phys. Rev. D* **68**, 085007 (2003).
- [10] S. Kobayashi, K. Koyama and J. Soda, *Phys. Rev. D* **65**, 064014 (2002).
- [11] A. Melfo, N. Pantoja and A. Skirzewski, *Phys. Rev. D* **67**, 105003 (2003).
- [12] R. Ghoroku and M. Yahiro, “Instability of thick brane worlds”, hep-th/0305150.
- [13] K.A. Bronnikov and B.E. Meierovich, “A general thick brane supported by a scalar field”, *Grav. & Cosmol.* **9**, 313 (2003); gr-qc/0402030.

-
- [14] S.T. Abdyrakhmanov, K.A. Bronnikov and B.E. Meierovich, “Uniqueness of RS2 type thick branes supported by a scalar field”, *Grav. & Cosmol.* **11**, 82 (2005); gr-qc/0503055.
- [15] I. Olasagasti and A. Vilenkin, “Gravity of higher-dimensional global defects”, *Phys. Rev. D* **62**, 044014 (2000); hep-th/0003300.
- [16] E. Roessl and M. Shaposhnikov, “Localizing gravity on a ’t Hooft-Polyakov monopole in seven dimensions”, *Phys. Rev. D* **66**, 084008 (2002); hep-th/0205320.
- [17] K.A. Bronnikov and B.E. Meierovich, “Gravitating global monopoles in extra dimensions and the braneworld concept.” *Sov. Phys. JETP* **101**, 6, 1036 (2005); *Zh. Eksp. Teor. Fiz.* **128**, 1184 (2005); gr-qc/0507032.
- [18] K.A. Bronnikov, B.E. Meierovich and S.T. Abdyrakhmanov, “Global topological defects in extra dimensions and the brane-world concept”, *Grav. & Cosmol.* **12**, 109 (2006).
- [19] I.I. Kogan, S. Mouslopoulos, A. Papazoglou and G. Ross. “Multigravity in six dimensions: Generating bounces with flat positive tension branes”, hep-th/0107086.
R. Koley and S. Kar, “Braneworlds in six dimensions: new models with bulk scalars,” *Class. Quantum Grav.* **24**, 79 (2007).
G. Kofinas and T.N. Tomaras, “Gravitating defects of codimension-two”, hep-th/0702010.
S. Kanno and J. Soda. “Quasi-thick Codimension 2 Braneworld”, hep-th/0404207.
- [20] K. Benson and I. Cho, “ A universe in a global monopole”, hep-th/0104067.
- [21] I. Cho and A. Vilenkin, “Spacetime structure of an inflating global monopole”, gr-qc/9708005
- [22] Y. Brihaye and T. Delsate. “Inflating branes inside hyper-spherically symmetric defects”, *Class. Quantum Grav.* **24**, 1279 (2007).
- [23] J.M. Cline, J. Descheneau, M. Giovannini and J. Vinet, “Cosmology of codimension-two braneworlds”, hep-th/0304147v2.